PHOTONICS Research

Second-order interference of true thermal light from a warm atomic ensemble in two independent unbalanced interferometers

Jiho Park, Heonoh Kim, and Han Seb Moon*

Department of Physics, Pusan National University, Geumjeong-Gu, Busan 46241, Republic of Korea
**Corresponding author: hsmoon@pusan.ac.kr*

Received 13 July 2020; revised 5 November 2020; accepted 15 November 2020; posted 18 November 2020 (Doc. ID 402574); published 23 December 2020

We report the demonstration of a second-order interference experiment by use of thermal light emitted from a warm atomic ensemble in two spatially separated unbalanced Michelson interferometers (UMIs). This novel multipath correlation interference with thermal light has been theoretically proposed by Tamma [New J. Phys. 18, 032002 (2016)]. In our experiment, the bright thermal light used for second-order interference is superradiantly emitted via collective two-photon coherence in Doppler-broadened cascade-type ^{87}Rb atoms. Owing to the long coherence time of the thermal light from the atomic ensemble, we observe its second-order interference in the two independent UMIs by means of time-resolved coincidence detection. The temporal waveforms of the interfering thermal light in the two spatially separated UMIs exhibit similarities with the temporal two-photon waveform of time–energy entangled photon pairs in Franson interferometry. Our results can contribute toward a better understanding of the relation between first- and second-order interferences that are at the heart of photonics-based quantum information science.

https://doi.org/10.1364/PRJ.402574

1. INTRODUCTION

Two-photon interference (TPI) lies at the heart of quantum optics research and quantum information applications such as quantum communication, quantum simulation, quantum computing, and quantum metrology [1–4]. In particular, Franson interference beyond the single-photon coherence length in twin nonlocal unbalanced interferometry (UI) experiments is considered a counterintuitive phenomenon from the viewpoint of classical physics [5–7]. The famous Franson interference experiment is important for understanding both the nonlocal nature of entanglement and the characteristics of time–energy entangled photons via coincidence detection according to the phase difference between the two two-photon amplitudes in UIs [5]. Thus far, several Franson interference experiments have been demonstrated with the use of entangled photon pairs, keeping in mind that Franson interference is regarded as evidence of the nonclassical nature of photon sources with time–energy entangled photons [5–10].

In this context, multipath correlation interference with thermal light based on twin UIs has been theoretically proposed by Tamma [11]. Unlike the Franson interference of entangled photon pairs, multipath correlation interference offers interesting points of the proposed interference. One is the path-length difference of each UI for emerging interference in no limitation beyond the coherence length of the thermal light, and another is that interference fringe is dependent on the path-length difference between the two UIs [11,12]. Recently, second-order temporal interference with pseudo-thermal light, using a rotating ground disk, has been experimentally demonstrated in two unbalanced Mach–Zehnder interferometers with one common long-path [13]. Although such an experimental method for pseudo-thermal light can imitate real thermal light with a high degree of fidelity, the realizable spectral bandwidth is limited to the range of a few megahertz because of the rotation speed, average grain spatial size of the ground disks, and the laser focal spot size [14]. Moreover, it is difficult to temporally maintain the phase difference between the two independent UIs with long-paths of hundreds of meters (spectral bandwidth of a few megahertz) because of the phase drift of the two UIs arising from thermal fluctuation, air flow, and acoustical vibration.

Here, we experimentally demonstrate second-order interference (SOI) with thermal light superradiantly emitted from warm ^{87}Rb atoms using two nonlocal unbalanced Michelson interferometers (UMIs). In our system, bright thermal light with a spectral bandwidth of the order of hundreds of megahertz is generated via spontaneous four-wave mixing (SFWM) in a Doppler-broadened cascade-type atomic ensemble [15,16]. The counting rate of the thermal light obtained via the two-photon transition of the cascade-type atomic system is

significantly higher than that of spontaneously emitted photons for one-photon transition because of the collective two-photon coherence effect [15]. In particular, we investigate the Franson-type interferometry of thermal light under the condition that the UMI path-length difference is larger than the coherence length of the thermal light. Moreover, we observe the SOI fringe according to the various conditions of the path-length difference between two independent UMIs.

2. EXPERIMENTAL SETUP

We briefly describe the setup used to realize SOI with thermal light (Fig. 1). Figure 1(a) shows the conceptual schematic of the Hanbury Brown–Twiss (HBT) experiment employed to observe the photon statistical properties with thermal light. From the measurement results of the HBT experiment, we can obtain the normalized second-order autocorrelation function $g^{(2)}(\tau)$ of thermal light, where τ denotes the time delay between two photon-counting events measured using two single-photon detectors (SPDs). The $g^{(2)}(0)$ value of thermal light is ~2, which is a characteristic photon statistical property of bunched photons, and the full-width at half-maximum (FWHM) of the $g^{(2)}(\tau)$ spectrum corresponds to the coherence time of the thermal light.

Meanwhile, as shown in Fig. 1(b), the proposed setup to realize SOI with thermal light includes two independent unbalanced Mach–Zehnder interferometers positioned after a beam splitter (BS). For coincidence detection between the two SPDs without one-photon interference of the thermal light, the optical path-length difference between the short and long arms of both unbalanced interferometers is set to be sufficiently longer than the coherence length of the incident thermal light. The conceptual schematic of the SOI experiment of Fig. 1(b) is the same as that of the Franson interference experiment except for the BS.

In this study, the thermal light for our experiment is obtained from a Doppler-broadened cascade-type atomic ensemble based on the $5S_{1/2} - 5P_{3/2} - 5D_{5/2}$ transition of ^{87}Rb, as shown in Fig. 2(a). Under the two-photon resonant condition with a far detuning frequency (δ) of 1 GHz from one-photon transitions, the superradiantly emitted photons are due to the collective two-photon coherence of the warm atomic ensemble with the two-photon resonant interaction [15].

As shown in Fig. 2(b), with the use of the counterpropagating geometry of the two contributing fields in the ^{87}Rb vapor cell, thermal light is generated in the phase-matched direction of the photon pairs from the Doppler-broadened atomic ensemble. Therefore, in our experiment, the superradiant photons emitted via the two-photon transition in the SFWM process are 20 times brighter than the scattered photons of the one-photon transition from the atomic ensemble. Relative to the idler photons, the signal photons of the $5P_{3/2} - 5D_{5/2}$ transition are more dominant of the thermal light due to the collective two-photon coherence effect because of low population of the $5P_{3/2}$ state and low single-emission fluorescence.

Figure 2(c) shows the temporal statistical spectrum of the signal photons as obtained from the HBT experiment. The spontaneous emission time of the photon is estimated to be ~1.9 ns, which is significantly shorter than the excited-state lifetime (26 ns) of the ^{87}Rb atom. This emission-time shortening of the thermal light can be understood as the coherent superposition of the two-photon amplitudes from different velocity classes in the Doppler-broadened atomic ensemble [17].

The normalized second-order correlation $g^{(2)}(0)$ was estimated to be ~1.75, which is close to the bunched light $g^{(2)}(0)$ value of 2 [14]. However, our SPD time jitter of ~0.4 ns is less than the $g^{(2)}(\tau)$ FWHM of 1.9 ns. The dominant cause

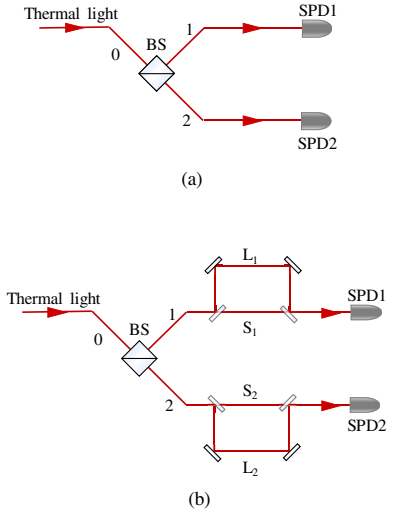

Fig. 1. Experimental configuration. (a) HBT experiment. (b) SOI with two independent unbalanced Mach–Zehnder interferometers.

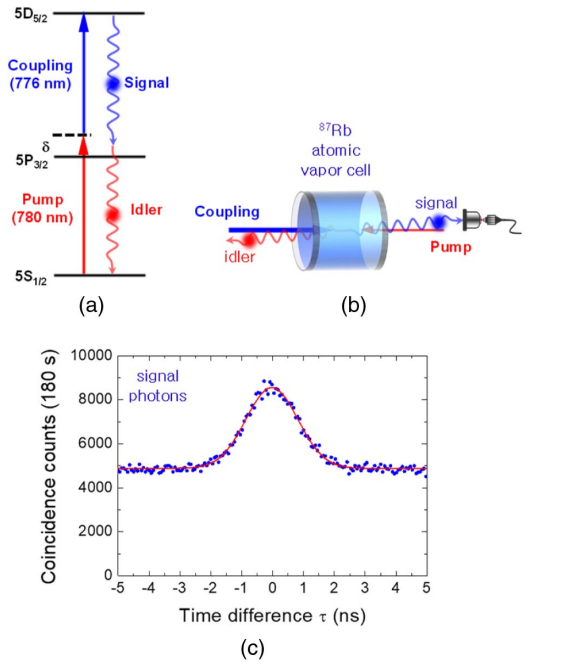

Fig. 2. Superradiant photons from Doppler-broadened cascade-type ^{87}Rb atoms. (a) Cascaded three-level atomic system of $5S_{1/2} - 5P_{3/2} - 5D_{5/2}$ transition of ^{87}Rb atoms. (b) Superradiant photon generation via SFWM process in the ^{87}Rb atomic vapor cell with counterpropagating pump and coupling lasers. (c) Temporal statistical spectrum of signal photons obtained via HBT setup for accumulation time of 180 s.

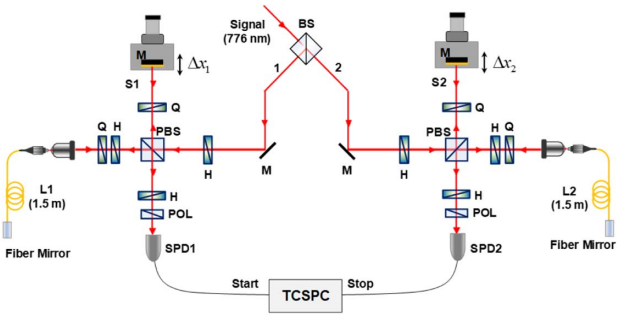

Fig. 3. Experimental setup for second-order interference with thermal light. SOI obtained with the use of unbalanced Michelson interferometers with large path difference: M, mirror; POL, polarizer; Q, quarter-wave plate; H, half-wave plate; PBS, polarizing beam splitter; SPD, single-photon detector.

limiting the $g^{(2)}(0)$ value is the time jitter of the employed SPDs. Considering the convolution of the $g^{(2)}(\tau)$ function and the time jitter (0.4 ns) of the employed SPDs, we can confirm that the calculated $g^{(2)}(0)$ value is identical to 1.75.

Figure 3 shows the experimental setup for SOI realization with the use of Franson-type interferometry consisting of two UMIs. In our experimental scheme, the bunched photons of the thermal light (signal photons) separated by the BS do not interact with each other and are spatially separated in the two UMIs.

The long (L_1 and L_2) paths of both UMI_1 and UMI_2 include an optical fiber mirror with a length of 1.5 m. The optical path length of the long path is estimated to be 4.8 m considering the refractive index of the optical fiber. We note here that the coherence length of the thermal light from the Doppler-broadened atomic ensemble is approximately 0.5 m, and thus, the optical path-length difference between the short and long arms of the UMI is sufficiently larger than the coherence length of the thermal light. The adjustable path length differences Δx_1 and Δx_2 of both short arms can be varied in steps of 0.1 μm with the use of two independent translator stages. Moreover, the SOI fringes were examined as a function of the Δx_1 and Δx_2 values of the short arms.

3. THEORY

The second-order correlation function $G^{(2)}(t_1, t_2)$ of the bunched thermal light in the two UMIs can be expressed as [11]

$$G^{(2)}(t_1, t_2) = G^{(1)}(t_1, t_1)G^{(1)}(t_2, t_2) + \eta|G^{(1)}(t_1, t_2)|^2, \quad (1)$$

where $G^{(1)}(t_1, t_2)$ denotes the first-order correlation function and t_1 and t_2 the detection times of these photons in SPD1 and SPD2, respectively. Moreover, thermal fraction coefficient η is related to the maximum second-order correlation value $G^{(2)}(t_1 = t_2)$ of our thermal light, including the time jitter of the employed SPDs. When the detection time difference $\tau \sim 0$, the $g^{(2)}(0)$ value as per Eq. (3) corresponds to the interference term. Parameter $g^{(2)}(0)$ can be simply expressed as

$$g^{(2)}(0) = 1 + \frac{\eta}{2}\left\{1 + \cos\left[\frac{\omega_0}{c}(L_1 - S_1) - (L_2 - S_2)\right]\right\}. \quad (2)$$

We can obtain sinusoidal SOI fringes according to the path-length difference between the long $(L_1 - L_2)$ and short $(S_1 - S_2)$ arms of both UMIs. Unlike the general Franson interference with entangled photon pairs, the SOI fringe with thermal light is dependent on the path-length difference between the two UMIs [6–9].

4. RESULTS

Figure 4 shows the temporal waveform of thermal light in Franson interferometry with twin nonlocal unbalanced interferometers. The temporal waveform was measured via coincidence counting for an accumulation time of 180 s using the TCSPC. For the first time, to the best of our knowledge, we could observe the time-resolved temporal waveform of thermal light from a warm atomic ensemble in both UMIs.

We note that the temporal waveform of thermal light consists of two side peaks due to the long–short (L_1S_2 and L_2S_1) path mismatch of the UMIs and the central interference peak at $\tau = 0$. We can infer that the two side peaks are phase-independent; however, the central interference peak is phase-sensitive according to the path-length difference between UMI_1 and UMI_2. This central peak at $\tau = 0$ is related to the four cases of short–short (S_1S_2), long–long (L_1L_2), long–short (L_1S_2), and short–long (S_1L_2) paths. In particular, the contribution at the central peak via both the L_1S_2 and S_1L_2 paths is due to temporally separated thermal photons, with the temporal separation arising from the time difference between the short and long arms of both UMIs.

The spectral feature of the three peaks is identical to the autocorrelation function curve of the thermal light from the warm atomic ensemble [Fig. 2(c)]. The magnitude of the central peak is approximately two times larger than those of both side peaks. In Fig. 4, the red box represents the 2.5 ns temporal window used for measuring the SOI fringes as a function of Δx_1 and Δx_2. Here, the detection time difference (ΔT) between the short and long paths is 16 ns, corresponding to the optical path lengths of both the long arms $(L_1 = L_2)$. We note that the time difference between the short and long arms of the UMI is sufficiently larger than the coherence time

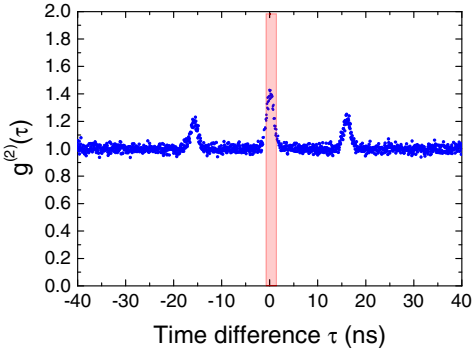

Fig. 4. Temporal waveform of real thermal light in Franson-type interferometer from Doppler-broadened cascade-type ^{87}Rb atoms.

of the thermal light. Interestingly, the temporal waveforms of the thermal light in the two spatially separated UMIs are similar to the temporal two-photon waveform of time–energy entangled photon pairs for Franson interferometry with twin nonlocal unbalanced interferometers [10].

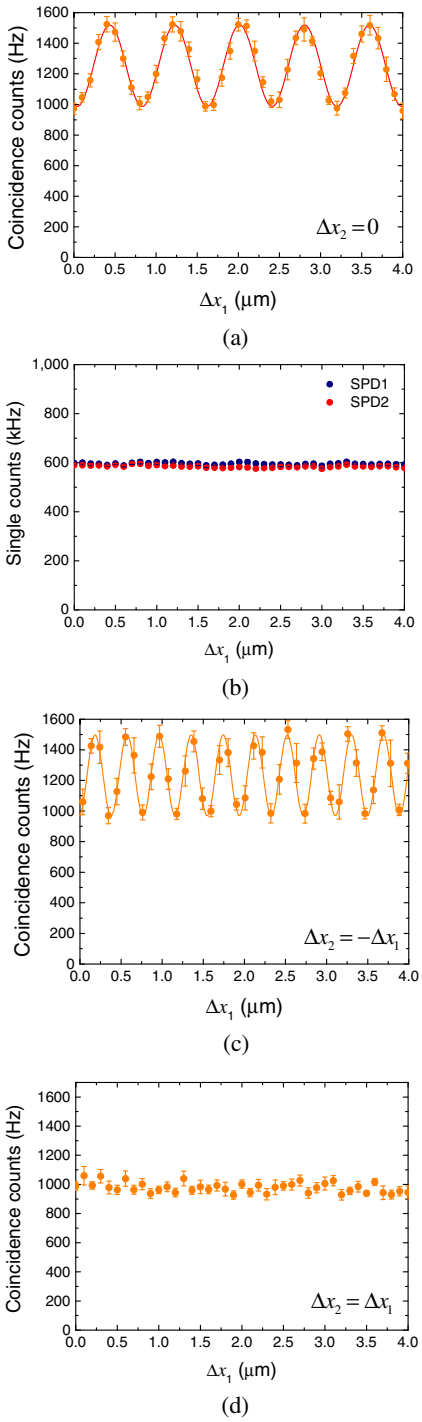

Fig. 5. Second-order interference with thermal light in two unbalanced Michelson interferometers. (a) SOI fringe of thermal light as a function of Δx_1 with fixed Δx_2 (coincidence detection of both SPDs). (b) Absence of first-order interference fringes in both SPD1 (blue circles) and SPD2 (red circles) as a function of Δx_1 or Δx_2. (c) SOI fringe as a function of Δx_1 when Δx_1 and Δx_2 are varied equally in opposite directions ($\Delta x_2 = -\Delta x_1$). (d) Absence of SOI fringe when Δx_1 and Δx_2 are varied equally along the same direction ($\Delta x_1 = \Delta x_2$).

In our experiment, we varied Δx_1 and Δx_2 of the short arms by using the translator stages (shown in Fig. 3) to investigate the SOI fringe variation according to the path-length difference of both UMIs. Figure 5(a) shows the sinusoidal SOI fringe of the thermal light from the warm atomic ensemble as a function of Δx_1 under the fixed short-path condition of SPD2 ($\Delta x_2 = 0$). The SOI fringe visibility was found to be 0.22 ± 0.01 and the fringe period was estimated to be 0.78 ± 0.05 μm from the sinusoidal fitting of the measured data points. For the observation of the SOI fringe of the thermal light, we measured the coincidence counting of both SPDs with a 2.5 ns coincidence window.

However, because the path-length difference between both arms of both UMIs is 10 times longer than the coherence length of the thermal light, one-photon interference fringes of the thermal light are not observed in SPD1 and SPD2, as indicated by the single counts in Fig. 5(b).

For the case in which the translator stages are moved equal distances in opposite directions ($\Delta x_1 = -\Delta x_2$), Fig. 5(c) shows the SOI fringe as a function of Δx_1. The visibility and period of the SOI fringe are estimated to be 0.22 ± 0.02 and 0.36 ± 0.05 μm, respectively. This SOI fringe exhibits a period that is half that in Fig. 5(a), with only a change in Δx_1 ($\Delta x_2 = 0$). This is because the phase difference in Eq. (2) is due to the adjustable path-length difference ($\Delta x_1 - \Delta x_2$) between the both UMIs.

Here, we note that the relative ratio of the coincidence window and the SPDs time jitter to the coherence time of the thermal light affects the visibility of the SOI fringe. Although the coincidence window is larger than the coherence time of the thermal light, we can clearly observe sinusoidal SOI fringes in Figs. 5(a) and 5(c). The SOI visibility is estimated to be 22%, and it is limited by the time jitter of the employed SPDs and the coincidence window.

On the other hand, in the case of both stages moving in the same direction ($\Delta x_1 = \Delta x_2$), the path-length difference between UMI_1 and UMI_2 is zero, and thus the phase difference in Eq. (2) is zero. Therefore, in Fig. 5(d), we can confirm the absence of SOI fringes when both Δx_1 and Δx_2 move in the same direction. These results highlight the features of the sinusoidal SOI fringes from the thermal light in comparison with the original Franson interference with entangled photon pairs.

5. CONCLUSION

In conclusion, we experimentally demonstrate the SOI phenomenon with thermal light generated from a cascade-type warm atomic ensemble via collective two-photon coherence. Using the bright thermal light from an atomic ensemble, for the first time to the best of our knowledge, we observed the temporal waveform of the thermal light in two independent UMIs. The temporal waveform of the thermal light is similar to the temporal two-photon waveform of time–energy entangled photon pairs in Franson interferometry, even though the path-length difference condition between both UMIs for the SOI fringes of the thermal light is opposite to that for the original Franson interference with an entangled photon pair.

We believe that the interesting difference between the second-order interferences with the time–energy entangled photon pairs and the bunched photons of thermal light can aid further advances in optical quantum information science.

Funding. National Research Foundation of Korea (2018R1A2A1A19019181, 2020M3E4A1080030); Institute for Information and Communications Technology Promotion (IITP-2020-0-01606).

Disclosures. The authors declare no conflicts of interest.

REFERENCES

1. Z. S. Yuan, X. H. Bao, C. Y. Lu, J. Zhang, C. Z. Peng, and J. W. Pan, "Entangled photons and quantum communication," Phys. Rep. **497**, 1–40 (2010).
2. I. M. Georgescu, S. Ashhab, and F. Nori, "Quantum simulation," Rev. Mod. Phys. **86**, 153–185 (2014).
3. J. L. O'Brien, "Optical quantum computing," Science **318**, 1567–1570 (2007).
4. V. Giovannetti, S. Lloyd, and L. Maccone, "Advances in quantum metrology," Nat. Photonics **5**, 222–229 (2011).
5. J. D. Franson, "Bell inequality for position and time," Phys. Rev. Lett. **62**, 2205–2208 (1989).
6. Z. Y. Ou, X. Y. Zou, L. J. Wang, and L. Mandel, "Observation of nonlocal interference in separated photon channels," Phys. Rev. Lett. **65**, 321–324 (1990).
7. J. Brendel, E. Mohler, and W. Martienssen, "Time-resolved dual-beam two-photon interferences with high visibility," Phys. Rev. Lett. **66**, 1142–1145 (1991).
8. H. Jayakumar, A. Predojević, T. Kauten, T. Huber, G. S. Solomon, and G. Weihs, "Time-bin entangled photons from a quantum dot," Nat. Commun. **5**, 4251 (2014).
9. M. Peiris, K. Konthasinghe, and A. Muller, "Franson interference generated by a two-level system," Phys. Rev. Lett. **118**, 030501 (2017).
10. J. Park, D. Kim, H. Kim, and H. S. Moon, "High-visibility Franson interference of time-energy entangled photon pairs from warm atomic ensemble," Opt. Lett. **44**, 3681–3684 (2019).
11. V. Tamma and J. Seiler, "Multipath correlation interference and controlled-not gate simulation with a thermal source," New J. Phys. **18**, 032002 (2016).
12. V. Tamma, "The physics of thermal light second-order interference beyond coherence," Phys. Scr. **93**, 124010 (2018).
13. Y. S. Ihn, Y. Kim, V. Tamma, and Y.-H. Kim, "Second-order temporal interference with thermal light: interference beyond the coherence time," Phys. Rev. Lett. **119**, 263603 (2017).
14. J. Mika, L. Podhora, L. Lachman, P. Obšil, J. Hloušek, M. Ježek, R. Filip, and L. Slodička, "Generation of ideal thermal light in warm atomic vapor," New J. Phys. **20**, 093002 (2018).
15. J. Park, T. Jeong, H. Kim, and H. S. Moon, "Time-energy entangled photon pairs from Doppler-broadened atomic ensemble via collective two-photon coherence," Phys. Rev. Lett. **121**, 263601 (2018).
16. J. Park, H. Kim, and H. S. Moon, "Polarization-entangled photons from a warm atomic ensemble using a Sagnac interferometer," Phys. Rev. Lett. **122**, 143601 (2019).
17. Y.-S. Lee, S. M. Lee, H. Kim, and H. S. Moon, "Single-photon superradiant beating from a Doppler-broadened ladder-type atomic ensemble," Phys. Rev. A **96**, 063832 (2017).